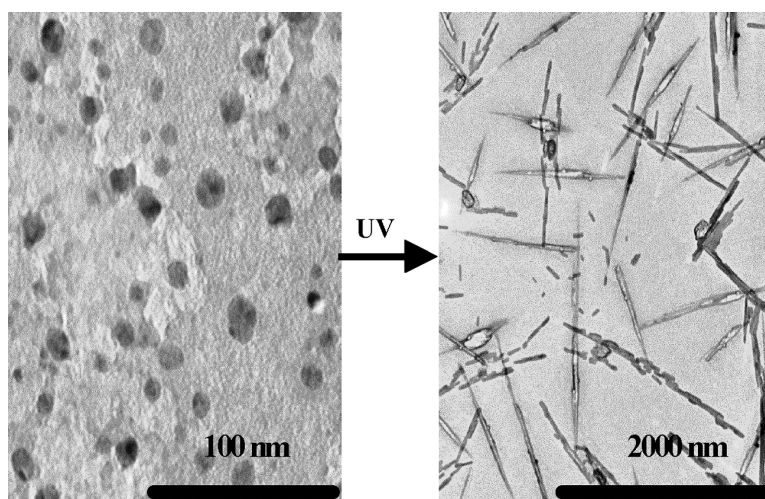Letter

Photodestructible Vesicles

Julian Eastoe, Ana Vesperinas, Anne-Carole Donnewirth, Paul Wyatt, Isabelle Grillo, Richard K. Heenan, and Sean Davis

More About This Article

Additional resources and features associated with this article are available within the HTML version:

- Supporting Information
- Links to the 9 articles that cite this article, as of the time of this article download
- Access to high resolution figures
- Links to articles and content related to this article
- Copyright permission to reproduce figures and/or text from this article

View the Full Text HTML

Langmuir
The ACS Journal of Surfaces and Colloids

Letters

Photodestructible Vesicles

Julian Eastoe,*,[†] Ana Vesperinas,[†] Anne-Carole Donnewirth,[†] Paul Wyatt,[†] Isabelle Grillo,[‡]
Richard K. Heenan,[§] and Sean Davis[†]

School of Chemistry, University of Bristol, Bristol BS8 1TS, U.K., Institut Max-von-Laue-Paul-Langevin,
BP 156-X, F-38042 Grenoble, Cedex, France, and ISIS-CCLRSC, Rutherford Appleton Laboratory,
Chilton, Oxon OX11 0QX, U.K.

Stable vesicles are formed in a 1.4 wt % solution comprising a 1:3 mixture of the anionic photodestructible surfactant sodium 4-hexylphenylazosulfonate (C_6PAS) and inert cationic cetyltrimethylamonium bromide (CTAB). UV irradiation drives an irreversible breakdown of the mixed C_6PAS/CATB vesicles, owing to the selective degradation of C_6PAS. A light-induced transition from small spherical-like polydisperse vesicles to long needle-like aggregation is observed.

Introduction

Vesicles are surfactant-based systems forming enclosed shells, which are often thought of as model biological membranes.[1] Previous studies have shown that thermodynamically stable vesicles form spontaneously on mixing aqueous solutions of synthetic cationic and anionic single-tailed surfactants in certain molar ratios.[2–6] Vesicles have been used as capsules for drug delivery[7] and as microreactors for the synthesis of magnetic nanoparticles[8] and functional polymer particles.[9–11] Recently, investigations have focused on modification and control over vesicle aggregation via changes in electrostatic interactions.[5,12] Light has also been used as a method to control vesicle stability;[13–16] this is an attractive approach because it is not necessary to change thermodynamic variables or the system chemical composition. UV–vis irradiation has been employed to achieve reversible control over vesicle formation[14] and also vesicle-to-micelle transitions via cis–trans photoisomerization of a surfactant.[15]

Photodestructible surfactants offer the possibility of an efficient and irreversible change in colloidal and aggregation properties. Studies involving an anionic photolyzable surfactant, sodium 4-hexylphenylazosulfonate (C_6PAS, structure shown in Supporting Information), showed that UV light can provoke the breakdown of microemulsions formulated from mixtures with inert Aerosol-OT.[17,18] Here, the concept of photodestructible

* Corresponding author. E-mail: julian.eastoe@bris.ac.uk.
† University of Bristol.
‡ Institut Max-von Laue-Paul-Langevin.
§ ISIS-CCLRC, Rutherford Appleton Laboratory.

(1) Singer, S. J.; Nicolson, G. L. *Science* **1972**, *175*, 720.
(2) Yatcilla, M. T.; Herrington, K. L.; Brasher, L. L.; Kaler, E. W. *J. Phys. Chem.* **1996**, *100*, 5874.
(3) Kaler, E. W.; Herrington, K. L.; Murthy, A. K. *J. Phys. Chem.* **1992**, *96*, 6698.
(4) Hao, J.; Yuan, Z.; Liu, W.; Hoffmann, H. *J. Phys. Chem.* **2004**, *108*, 5105.
(5) Brasher, L. L.; Kaler, E. W. *Langmuir* **1996**, *12*, 6270.
(6) Bergstrom, M.; Pedersen, J. S. *Langmuir* **1998**, *14*, 3754.
(7) Ostro, M. J.; Cullis, P. R. *Am. J. Hosp. Pharm.* **1989**, *46*, 1576.
(8) Yaacob, I. L.; Nunes, A. C.; Bose, A. *J. Colloid Interface Sci.* **1995**, *171*, 73.
(9) Yaacob, I. L.; Nunes, A. C.; Shah, D. O. *J. Colloid Interface Sci.* **1994**, *168*, 289.
(10) Shimomura, M.; Kunitake, T. *J. Am. Chem. Soc.* **1982**, *104*, 1982.
(11) Moss, R. A.; Bizzigott, G. O. *J. Am. Chem. Soc.* **1981**, *103*, 6512.

(12) Walker, S. A.; Zasadzinski, J. A. *Langmuir* **1997**, *13*, 5076.
(13) Veronese, A.; Berclaz, N.; Luisi, P. L. *J. Phys. Chem. B* **1998**, *102*, 7078.
(14) (a) Sakai, H.; Matsumura, A.; Yokoyama, S.; Saji, T.; Abe, M. *J. Phys. Chem. B* **1999**, *103*, 10737. (b) Hubbard, F. P., Jr.; Santonicola, G.; Kaler, E. W.; Abbott, N. L. *Langmuir* **2005**, *21*, 6131.
(15) Eastoe, J.; Sanchez-Dominguez, M.; Wyatt, P.; Beeby, A.; Heenan, R. K. *Langmuir* **2002**, *18*, 7837.
(16) Eastoe, J.; Sanchez-Dominguez, M.; Wyatt, P.; Orr-Ewing, A. J.; Heenan, R. K. *Langmuir* **2004**, *20*, 6120.
(17) Eastoe, J.; Sanchez-Dominguez, M.; Cumber, H.; Wyatt, P.; Heenan, R. K. *Langmuir* **2004**, *20*, 1120.
(18) Eastoe, J.; Sanchez-Dominguez, M.; Cumber, H.; Burnett, G.; Wyatt, P.; Heenan, R. K. *Langmuir* **2003**, *19*, 6579.

vesicles is explored by employing mixtures of C_6PAS and inert cationic cetyltrimethylamonium bromide (CTAB). The idea is that these functionalized vesicles can be broken down by specific photodegradation of C_6PAS alone. The photochemistry of C_6PAS has been extensively characterized,[16,17,19,20] as outlined in Supporting Information, and there are two dominant photoproducts—the nonsurface active alkane hexylbenzene and the weakly surface-active 4-hexylphenol.
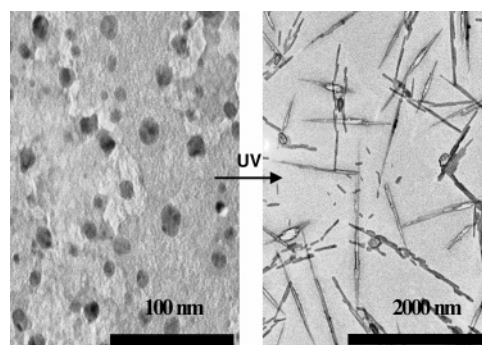
Experimental Section

Materials. Sodium 4-hexylphenylazosulfonate (C_6PAS, MW = 292.3) was synthesized, purified, and characterized as outlined elsewhere.[17-19] Cationic surfactant cetyltrimethylammonium bromide (CTAB, MW = 364.45, Alfa Aesar, 98%) was recrystallized three times from a 1:1 mixture of ethanol and acetone. Stock surfactant solutions, at appropriate concentrations, were prepared in D_2O (Fluorochem, 99.9% D atom), and these were then equilibrated at room temperature for 1 day in the dark. Vesicle solutions were made up at a mole ratio of 1:3 CTAB/C_6PAS from these stocks by dilution and mixing in the desired ratios. The initial systems were at 1.4 wt % total surfactant, which were also diluted to 1.05 wt %. D_2O was used as the solvent so that small-angle neutron scattering experiments could be performed. This change meant that the phase-stability region shifted to 40 °C rather than 25 °C if H_2O were used.[3,5] All samples were incubated for at least 2 weeks at 40 °C before any further investigations.

Methods

Photoirradiation was carried out in quartz cells with an unfiltered 100 W high-pressure white source (Oriel). The irradiation time was a function of C_6PAS concentration, based on 270 min for an 80 mM solution. UV–vis spectroscopy (Unicam UV2) was used to follow the reaction and to ascertain that the photolysis of C_6PAS was complete. (See Supporting Information. For these systems, line broadening meant that ^1H NMR was less appropriate for this purpose.) Before analysis with transmission electron microscopy (TEM), small-angle neutron scattering (SANS), and dynamic light scattering (DLS), precautions were taken to avoid any unnecessary daylight exposure of the samples. Specimens for TEM were prepared by depositing a drop of solution onto Parafilm and then placing it over a 3 mm copper grid. After 1 min, the grid was removed, and excess solution was wicked away using filter paper. The fully dried samples were imaged at 120 kV in a model JEOL JEM 1200 EX transmission electron microscope. SANS experiments were carried out on the D22 diffractometer at ILL (Grenoble, France) using a neutron wavelength of $\lambda = 10$ Å at two different detector distances to cover a Q range of $0.006 \rightarrow 0.37$ Å^{-1}. Absolute intensities for $I(Q)$ (cm^{-1}) were determined to within ±5% by measuring the incoherent scattering from 1 mm of H_2O. Samples were preequilibrated in 2 mm quartz cuvettes, at 40 °C for 40 min, prior to running the measurements at this temperature. Curve-fitting analysis was performed as described in Supporting Information, and the scattering laws are given elsewhere.[15,21] DLS was performed on a Brookhaven Zeta Plus Particle Size Analysis rig at a scattering angle of 90°. The samples were equilibrated and run at 40 °C. The intensity autocorrelation functions were analyzed by the method of cumulants.

Results and Discussion

TEM images (Figure 1) and photographs (Figure 2 inset) of the samples before and after irradiation reveal significant effects of UV on the microscopic state and macroscopic appearance of the samples. C_6PAS displays an intense UV absorption (λ_{max} = 308 nm, Supporting Information) and is responsible for the bright-

(19) Nuyken, O.; Voit, B. *Macromol. Chem. Phys.* **1997**, *198*, 2337.

(20) Mezger, T.; Nuyken, O.; Meindl, K.; Wokaun, A. *Prog. Org. Coat.* **1996**, *29*, 147.

(21) (a) Heenan, R. K. Fish Data Analysis Program; Report RAL-89-129; Rutherford Appleton Laboratory; CCLRC: Didcot, U.K., 1989. (b) Kotlarchyk, M.; Ritzau, S. M. *J. Appl. Crystallogr.* **1991**, *24*, 753.

Figure 1. Photoinduced changes in aggregation. TEM images for 1.4 wt % 1:3 CTAB/C_6PAS systems in D_2O (a) before and (b) after irradiation.
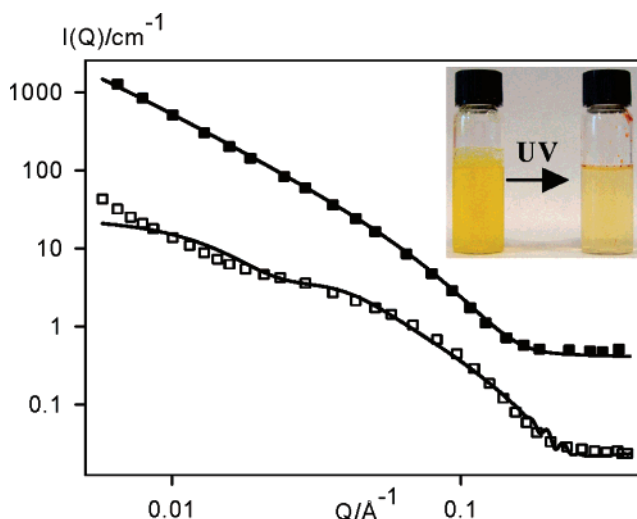
Figure 2. SANS data from 1.4 wt % 1:3 CTAB/C_6PAS in D_2O before ($\square$) and after ($\blacksquare$, $I(Q) \times 50$) irradiation. The fits shown as lines are for hollow vesicles in the preirradiated state and sheetlike aggregates in the post-irradiated state. The inset shows solutions before and after irradiation.

yellow color exhibited by the catanionic mixture prior to irradiation (Figure 2). The milky appearance of the preirradiated solution might be due to the presence of vesicles. After irradiation, the solution turned a cloudy, slightly brownish color, with dispersed oily brown droplets and no appreciable absorption maximum (Supporting Information). This suggests that the initial photosurfactant is essentially absent after sufficient exposure. The presence of CTAB did not appear to affect the C_6PAS photolysis.

Significant photoinduced changes in aggregation were confirmed with TEM. Figure 1 shows a clear transition from small spheroidal polydisperse particles to much larger needlelike structures: size range values are listed in Table 1. On the basis of photochemical studies (Supporting Information and refs 17–20), the post-irradiation structures consist of mixed CTAB/hexylphenol/hexyl benzene aggregates, where alkylphenol is the dominant photoproduct.

SANS measurements were carried out to study the effect of UV irradiation on aggregation (Figure 2), and large changes in the scattering are evident. In the preirradiated state at 1.4 wt %, the initial SANS data were best fitted by a model for polydisperse single-shell hollow spherical vesicles with an overall radius of $R_2 = 9.2$ nm (Table 1, polydispersity 0.36). These scattering laws are detailed elsewhere.[15] Using absolute scattering intensities to account quantitatively for the scattering, this analysis of preirradiated samples was consistent with the presence of a D_2O

Table 1. Particle Sizing Method Comparisons for 1:3 CTAB/C$_6$PAS Mixtures in D$_2$O at 1.05 and 1.4 wt % before and after Irradiation
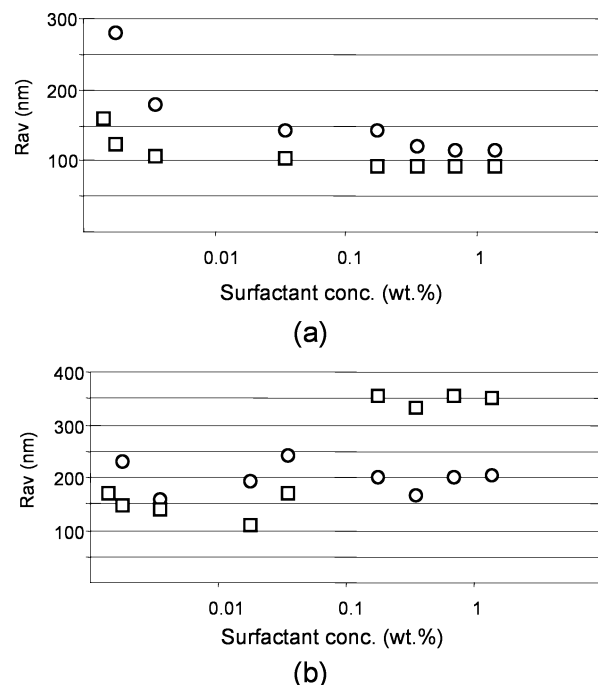
wt %		DLS $R_{av}{}^a$	SANS R_1	R_2	δ	t	TEM R_{av}	t
1.05	NI	99.9	12.4	15.1	2.7		4−23	
	IR	156.9				3.4		30−40
1.40	NI	92.9	7.0	9.2	2.2		2−12	
	IR	350.8				3.4		30−50

^{a} Polydispersity: 0.22−0.31. NI/IR: preirradiated/postirradiated condition. R_{av}(nm): particle average radius. $R_2 = R_1 + \delta$ (nm) with R_2, R_1, and δ being the external radius, internal cavity radius, and shell thickness from the Schultz polydisperse spherical hollow shell model described in ref 15, respectively. Parameter t(nm) is the sheet thickness in the Kotlarchyk model.[21b]

internal core, surrounded by an H-surfactant shell, which was dispersed in a D$_2$O continuum. However, the SANS curve for the post-irradiated samples could not be fitted by this hollow vesicle scattering law. Instead, it could be adequately described by the model proposed by Kotlarchyk et al.[21b] for a semi-infinite stack of monodisperse oriented sheets with an internal sheet spacing of 3.4 nm. The fitting parameters are given in Table 1. These SANS data and analyses reveal a transition from polydisperse spherical vesicles to much larger long, thin sheets. At first sight, the needlelike post-irradiation morphology seen by TEM (Figure 1) and the scattering law for oriented sheets employed to analyze the related SANS data (Figure 2) appear to be at odds. However, over the experimental Q range employed here, the upper length-scale resolution for SANS is ~100 nm, whereas the lower resolution of TEM at this magnification is about 3 nm. Hence, the two methods essentially report on different aspects of the same structure, with SANS being sensitive to internal details and the sheet separation and TEM being sensitive to the overall structures of the post-irradiated aggregates.[22]

Particle sizing analysis by DLS was also performed as shown in Figure 3, and the results are compared to those of the two other methods in Table 1. As shown in Figure 3, the measured diameters remain essentially constant for the two systems before and after irradiation, at least for dilutions down to 0.1 wt %. The trends are consistent between the methods, and on dilution, the preirradiated vesicles appear to swell, whereas the post-irradiated sheets shrink. For the samples around 1 wt %, the apparent increase in diameter post-irradiation seen by DLS is consistent with the increased sizes seen by TEM owing to the changes in composition mentioned above. (Note the scale bars in Figure 1.) SANS and TEM give very similar dimensions for the aggregation structures. (Note that the internal sheet thickness is difficult to estimate from TEM images.) However, by DLS the vesicles appear to be about 10 times larger as compared to the results from TEM and/or SANS. The cumulant analysis method determines an

Figure 3. DLS measurements of the average radius (R_{av}) for 1:3 CTAB/C$_6$PAS mixtures in D$_2$O at 1.05 wt % (○) and 1.40 wt % (□) before (a) and after (b) irradiation as a function of dilution.

average particle size, which here also has a relatively high polydispersity (0.36), and this may also contribute to the discrepancies because light scattering intensities are weighted to larger sizes.

Summary

Spontaneous vesicle formation was observed in these dilute aqueous catanionic mixtures comprising photodestructible anionic surfactant C$_6$PAS. This behavior is reminiscent of that known for mixtures of inert cationic and anionic mixtures.[2,3,5] TEM, SANS, and DLS experiments have shown that these vesicles can be broken down by the action of UV light, owing to the selective photolysis of C$_6$PAS. This study provides proof-of-principle and paves the way to develop more sophisticated photodestructible vesicles, which may find uses in specialist light-triggered release applications.

Supporting Information Available: Details of C$_6$PAS photochemistry, TEM, SANS, and DLS experiments as well as data treatment and analysis. This material is available free of charge via the Internet at http://pubs.acs.org.

LA052882R

(22) To make an analogy to a book, SANS is sensitive to the nanoscale spacing between sheets (pages), whereas TEM sees the overall micrometer-scale structure (book).